

**VAPOR-EXPLOSION EXPERIMENTS  
WITH SUBCOOLED FREON**

**by**

**Robert E. Henry and Louis M. McUumber**

BASE TECHNOLOGY



U of C - AUA - USERDA

---

**ARGONNE NATIONAL LABORATORY, ARGONNE, ILLINOIS**  
**Prepared for the U. S. ENERGY RESEARCH**  
**AND DEVELOPMENT ADMINISTRATION**  
**under Contract W-31-109-Eng-38**

The facilities of Argonne National Laboratory are owned by the United States Government. Under the terms of a contract (W-31-109-Eng-38) between the U. S. Energy Research and Development Administration, Argonne Universities Association and The University of Chicago, the University employs the staff and operates the Laboratory in accordance with policies and programs formulated, approved and reviewed by the Association.

#### MEMBERS OF ARGONNE UNIVERSITIES ASSOCIATION

The University of Arizona	Kansas State University	The Ohio State University
Carnegie-Mellon University	The University of Kansas	Ohio University
Case Western Reserve University	Loyola University	The Pennsylvania State University
The University of Chicago	Marquette University	Purdue University
University of Cincinnati	Michigan State University	Saint Louis University
Illinois Institute of Technology	The University of Michigan	Southern Illinois University
University of Illinois	University of Minnesota	The University of Texas at Austin
Indiana University	University of Missouri	Washington University
Iowa State University	Northwestern University	Wayne State University
The University of Iowa	University of Notre Dame	The University of Wisconsin

#### NOTICE

This report was prepared as an account of work sponsored by the United States Government. Neither the United States nor the United States Energy Research and Development Administration, nor any of their employees, nor any of their contractors, subcontractors, or their employees, makes any warranty, express or implied, or assumes any legal liability or responsibility for the accuracy, completeness or usefulness of any information, apparatus, product or process disclosed, or represents that its use would not infringe privately-owned rights. Mention of commercial products, their manufacturers, or their suppliers in this publication does not imply or connote approval or disapproval of the product by Argonne National Laboratory or the U. S. Energy Research and Development Administration.

Printed in the United States of America  
Available from  
National Technical Information Service  
U. S. Department of Commerce  
5285 Port Royal Road  
Springfield, Virginia 22161  
Price: Printed Copy \$4.50; Microfiche \$3.00

---

ANL-77-43

---

ARGONNE NATIONAL LABORATORY  
9700 South Cass Avenue  
Argonne, Illinois 60439

VAPOR-EXPLOSION EXPERIMENTS  
WITH SUBCOOLED FREON

by

Robert E. Henry and Louis M. McUmbert

Reactor Analysis and Safety Division

June 1977



## TABLE OF CONTENTS

	<u>Page</u>
ABSTRACT . . . . .	7
I. INTRODUCTION. . . . .	7
II. EXPERIMENTAL APPARATUS. . . . .	9
III. EXPERIMENTAL RESULTS . . . . .	9
IV. DISCUSSION OF RESULTS . . . . .	12
V. CONCLUSIONS. . . . .	14
APPENDIXES	
A. Experimental Data. . . . .	15
B. Results, Grouped by 10°C Increments of Oil Temperature. . . . .	28
REFERENCES . . . . .	29

## LIST OF FIGURES

<u>No.</u>	<u>Title</u>	<u>Page</u>
1.	Experimental Apparatus . . . . .	10
2.	Pressure-Time History for Freon-22 and Mineral-oil Undergoing Large-scale Interactions with $T_{oil} = 131^{\circ}C$ and $T_F = -41^{\circ}C$ . . . . .	11
3.	Pressure-Time History for Freon-22 and Mineral-oil Undergoing Large-scale Interactions with $T_{oil} = 140^{\circ}C$ and $T_F = -41^{\circ}C$ . . . . .	11
4.	Pressure-Time History for Freon-22 and Mineral-oil Undergoing Large-scale Interactions with $T_{oil} = 180^{\circ}C$ and $T_F = -41^{\circ}C$ . . . . .	11
5.	Pressure-Time History for Freon-22 and Mineral-oil Undergoing Large-scale Interactions with $T_{oil} = 190^{\circ}C$ and $T_F = -41^{\circ}C$ . . . . .	11
6.	Pressure-Time History for Freon-22 and Mineral-oil Undergoing Large-scale Interactions with $T_{oil} = 190^{\circ}C$ and $T_F = -60^{\circ}C$ . . . . .	12
7.	Pressure-Time History for Freon-22 and Mineral-oil Undergoing Large-scale Interactions with $T_{oil} = 190^{\circ}C$ and $T_F = -100^{\circ}C$ . . . . .	12
8.	Comparison between Interface-temperature Model and Experimental Results . . . . .	13
9.	Maximum Interaction Pressures as a Function of Interface Temperature . . . . .	13
10.	Maximum Interaction Pressures vs Interface Temperature. . . . .	14
A.1.	Experimental Data Records for Run 6-11-75: 1 +145 -72 . . . . .	16
A.2.	Experimental Data Records for Run 6-11-75: 5 +148 -68 . . . . .	16
A.3.	Experimental Data Records for Run 6-11-75: 6 +145 -92 . . . . .	16
A.4.	Experimental Data Records for Run 6-16-75: 1 +169 -110 . . . . .	16
A.5.	Experimental Data Records for Run 6-16-75: 4 +190 -111 . . . . .	17
A.6.	Experimental Data Records for Run 6-16-75: 5 +146 -77 . . . . .	17
A.7.	Experimental Data Records for Run 6-18-75: 1 +132 -58 . . . . .	17
A.8.	Experimental Data Records for Run 6-19-75: 1 +198 -128 . . . . .	17
A.9.	Experimental Data Records for Run 6-19-75: 3 +174 -120 . . . . .	18
A.10.	Experimental Data Records for Run 6-19-75: 4 +168 -95 . . . . .	18

## LIST OF FIGURES

<u>No.</u>	<u>Title</u>	<u>Page</u>
A.11.	Experimental Data Records for Run 6-19-75: 5 +156 -94 . . . . .	18
A.12.	Experimental Data Records for Run 7-10-75: 1 +160 -99 . . . . .	18
A.13.	Experimental Data Records for Run 7-10-75: 4 +163 -122 . . . . .	19
A.14.	Experimental Data Records for Run 7-15-75: 2 +180 -110 . . . . .	19
A.15.	Experimental Data Records for Run 7-15-75: 3 +178 -100 . . . . .	19
A.16.	Experimental Data Records for Run 7-15-75: 4 +178 -80 . . . . .	19
A.17.	Experimental Data Records for Run 7-15-75: 5 +180 -60 . . . . .	20
A.18.	Experimental Data Records for Run 7-15-75: 6 +161 -60 . . . . .	20
A.19.	Experimental Data Records for Run 7-16-75: 1 +190 -41 . . . . .	20
A.20.	Experimental Data Records for Run 7-16-75: 2 +190 -60 . . . . .	20
A.21.	Experimental Data Records for Run 7-16-75: 3 +192 -80 . . . . .	21
A.22.	Experimental Data Records for Run 7-17-75: 1 +190 -101 . . . . .	21
A.23.	Experimental Data Records for Run 7-18-75: 2 +190 -90 . . . . .	21
A.24.	Experimental Data Records for Run 7-23-75: 1 +150 -41 . . . . .	21
A.25.	Experimental Data Records for Run 7-23-75: 2 +170 -41 . . . . .	22
A.26.	Experimental Data Records for Run 7-23-75: 3 +182 -99 . . . . .	22
A.27.	Experimental Data Records for Run 7-23-75: 4 +190 -100 . . . . .	22
A.28.	Experimental Data Records for Run 7-23-75: 5 +190 -80 . . . . .	22
A.29.	Experimental Data Records for Run 7-24-75: 1 +190 -100 . . . . .	23
A.30.	Experimental Data Records for Run 7-24-75: 2 +190 -80 . . . . .	23
A.31.	Experimental Data Records for Run 7-24-75: 3 +190 -90 . . . . .	23
A.32.	Experimental Data Records for Run 7-24-75: 4 +131 -41 . . . . .	23
A.33.	Experimental Data Records for Run 7-25-75: 1 +180 -41 . . . . .	24
A.34.	Experimental Data Records for Run 7-25-75: 2 +160 -41 . . . . .	24
A.35.	Experimental Data Records for Run 7-25-75: 3 +180 -41 . . . . .	24
A.36.	Experimental Data Records for Run 7-25-75: 4 +140 -41 . . . . .	24
A.37.	Experimental Data Records for Run 7-25-75: 5 +195 -41 . . . . .	25
A.38.	Experimental Data Records for Run 7-25-75: 6 +185 -41 . . . . .	25
A.39.	Experimental Data Records for Run 7-25-75: 7 +175 -41 . . . . .	25

## LIST OF FIGURES

<u>No.</u>	<u>Title</u>	<u>Page</u>
A.40.	Experimental Data Records for Run 7-28-75: 1 +183 -41 . . . . .	25
A.41.	Experimental Data Records for Run 7-28-75: 2 +176 -41 . . . . .	26
A.42.	Experimental Data Records for Run 7-28-75: 3 +180 -41 . . . . .	26
A.43.	Experimental Data Records for Run 7-28-75: 4 +173 -41 . . . . .	26
A.44.	Experimental Data Records for Run 7-28-75: 5 +169 -41 . . . . .	26
A.45.	Experimental Data Records for Run 7-28-75: 6 +166 -41 . . . . .	27
A.46.	Experimental Data Records for Run 8-4-75: 3 +190 -100 . . . . .	27
A.47.	Experimental Data Records for Run 8-4-75: 4 +190 -90 . . . . .	27

## LIST OF TABLES

<u>No.</u>	<u>Title</u>	<u>Page</u>
I.	Homogeneous Nucleation for Freon-22 at 1 atm (0.1 MPa). . . . .	8
II.	Chronological List of Experiments . . . . .	15

# VAPOR-EXPLOSION EXPERIMENTS WITH SUBCOOLED FREON

by

Robert E. Henry and Louis M. McUmbert

## ABSTRACT

Vapor-explosion experiments were conducted in a well-wetted Freon-22 and mineral-oil system in which the initial temperature of both the Freon and the mineral oil were varied over a wide range. These experiments were specifically conducted to investigate the importance of interface temperature in determining the explosive behavior of a given system. The results clearly demonstrate that the interface temperature developed upon intimate liquid-liquid contact is a valid characterization of the explosive potential of a given system.

## I. INTRODUCTION

Explosive vapor formation, accompanied by destructive shock waves, can be produced when two liquids, at much different temperatures, are brought into intimate contact. A proposed analytical model<sup>1,2</sup> states that, (1) upon contact between the two liquid systems, the interface temperature must be greater than or equal to the limiting spontaneous nucleation temperature of that liquid-liquid system, and (2) the thermal boundary layer must be sufficiently developed to support a critical-size cavity. For time scales greater than  $10^{-12}$  s, the interface temperature upon contact of two semi-infinite masses, with constant thermal properties, can be related to the initial liquid temperatures by the equation<sup>3</sup>

$$T_i = \frac{T_h + T_c \sqrt{k_c \rho_c c_c / k_h \rho_h c_h}}{1 + \sqrt{k_c \rho_c c_c / k_h \rho_h c_h}},$$

where

$c$  = specific heat,

$k$  = thermal conductivity,

$T$  = temperature,

$\rho$  = density,

and the subscripts

c = cold liquid

h = hot liquid

and

i = interface.

The spontaneous nucleation behavior at the interface can either be heterogeneous or homogeneous in nature.<sup>4</sup> In either case, the critical-size cavities, which initiate the vaporization process, are produced by local density fluctuations within the cold liquid. For homogeneous conditions, the two liquids present a well-wetted system and the vapor embryos are produced entirely within the cold liquid. For heterogeneous conditions, which result from poor or imperfect wetting at the liquid-liquid interface, the critical-sized cavities are created at the interface at somewhat lower temperatures. The homogeneous nucleation rates for Freon-22 at 0.1 MPa (1 atm) are listed in Table I for various temperature levels.

A sequence of experiments, using Freon-22 and water, Freon-22 and mineral oil, and Freon-12 and mineral oil, have been performed to test this spontaneous nucleation premise.<sup>5</sup> For Freon-22 at its normal boiling point, the initial temperature of the water must be at least 77°C before the interface temperature equals or exceeds the minimum homogeneous nucleation value of 54°C (see Table I), and 84°C before the interface temperature equals 60°C, at which the homogeneous nucleation rate becomes truly explosive.<sup>2</sup> As illustrated in Ref. 5, the Freon-water test demonstrated explosive interactions for water temperatures considerably lower than this value, which was attributed to the heterogeneous nucleation characteristics of that particular system resulting from the poor wetting between Freon and water. However, the experimental data demonstrate a definite threshold behavior at a water temperature of about 45°C, and this value has been observed by other experimenters with the same fluids.<sup>6</sup> The Freon-mineral-oil systems exhibited excellent agreement with the interface-temperature model in which the spontaneous nucleation behavior is assumed to be homogeneous because of the affinity between Freons and oils.

TABLE I. Homogeneous Nucleation for Freon-22 at 1 atm (0.1 MPa)

Temperature, °C	Vapor Pressure, mPa	Surface Tension, 10 <sup>-3</sup> N/m	Critical Cavity Radius, 10 <sup>-10</sup> m	Nucleation Rate, sites/cm <sup>3</sup> ·s	Waiting Time per cm <sup>3</sup>
50	1.94	4.71	49	3.9 × 10 <sup>-18</sup>	8 × 10 <sup>9</sup> yr
52	2.03	4.46	44	2.0 × 10 <sup>-6</sup>	5.8 days
54	2.12	4.22	40	2.4 × 10 <sup>3</sup>	400 μs
56	2.23	3.97	36	7.2 × 10 <sup>10</sup>	10 <sup>-11</sup> s
58	2.32	3.73	32	1.6 × 10 <sup>16</sup>	6 × 10 <sup>-17</sup> s
60	2.43	3.49	29	3.7 × 10 <sup>20</sup>	3 × 10 <sup>-21</sup> s

The applicability of the interface temperature model was investigated<sup>7</sup> by varying the initial subcooling of the Freon in a Freon-22-water system. The intent of these experiments was to change the interface temperature by subcooling the Freon and observe the resulting changes in the explosive behavior of the system. The conclusion from these experiments was that the explosive behavior did not change with increasing Freon subcooling and, hence, with changing interface temperature. This system has two inherent disadvantages which tend to cloud the experimental results. The first is that the excellent thermal properties of the water, compared to those of the Freon, significantly reduce the sensitivity of the interface temperature to Freon subcooling. The second is that, since one is already dealing with a poorly wetted system, the wetting characteristics can be altered by changing the interface temperature, which, in turn, changes the heterogeneous nucleation temperature. To provide a more definitive test of the interface-temperature representation by subcooling the cold liquid, a system of Freon-22 and mineral oil, which presents a well-wetted system, was used in this set of experiments. In addition to the better wetting characteristics, the thermal conductivity, density, and specific heat of the mineral oil are less than those of the water. This results in a greater sensitivity of this system to changes in the initial subcooling of the Freon.

## II. EXPERIMENTAL APPARATUS

To investigate the relative importance of the interface temperature, experiments were conducted in two different manners. The first was performed with the Freon initially at its normal boiling point and mineral-oil temperatures ranging from 110 to 190°C in 10° increments. The second was carried out with the mineral-oil temperature held constant at 190°C and decreasing Freon temperatures from -41 to -140°C in 20° increments. The tests were carried out in the A-frame apparatus illustrated in Fig. 1, which is a facility similar to that discussed in Ref. 5. The principal exception between the facilities is that, in this case, the interaction vessel always contained the Freon and the hot oil was poured into the vessel. This change in contact configuration has little significance when the Freon-22 is saturated, but for subcooled Freon it provides a better experimental resolution for the initial Freon temperatures. The oil entered the interaction vessel through a rubber funnel, and high-speed motion pictures, at 1000 frames/s, were taken of the resulting interactions, along with analog recordings of the high-response piezoelectric transducers mounted in the vessel wall and of the piezoelectric force transducer that supported the vessel.

## III. EXPERIMENTAL RESULTS

For initial mineral-oil temperatures less than 130°C and initially saturated Freon, no explosive interactions were observed on the high-speed movies or the pressure-transducer recordings.

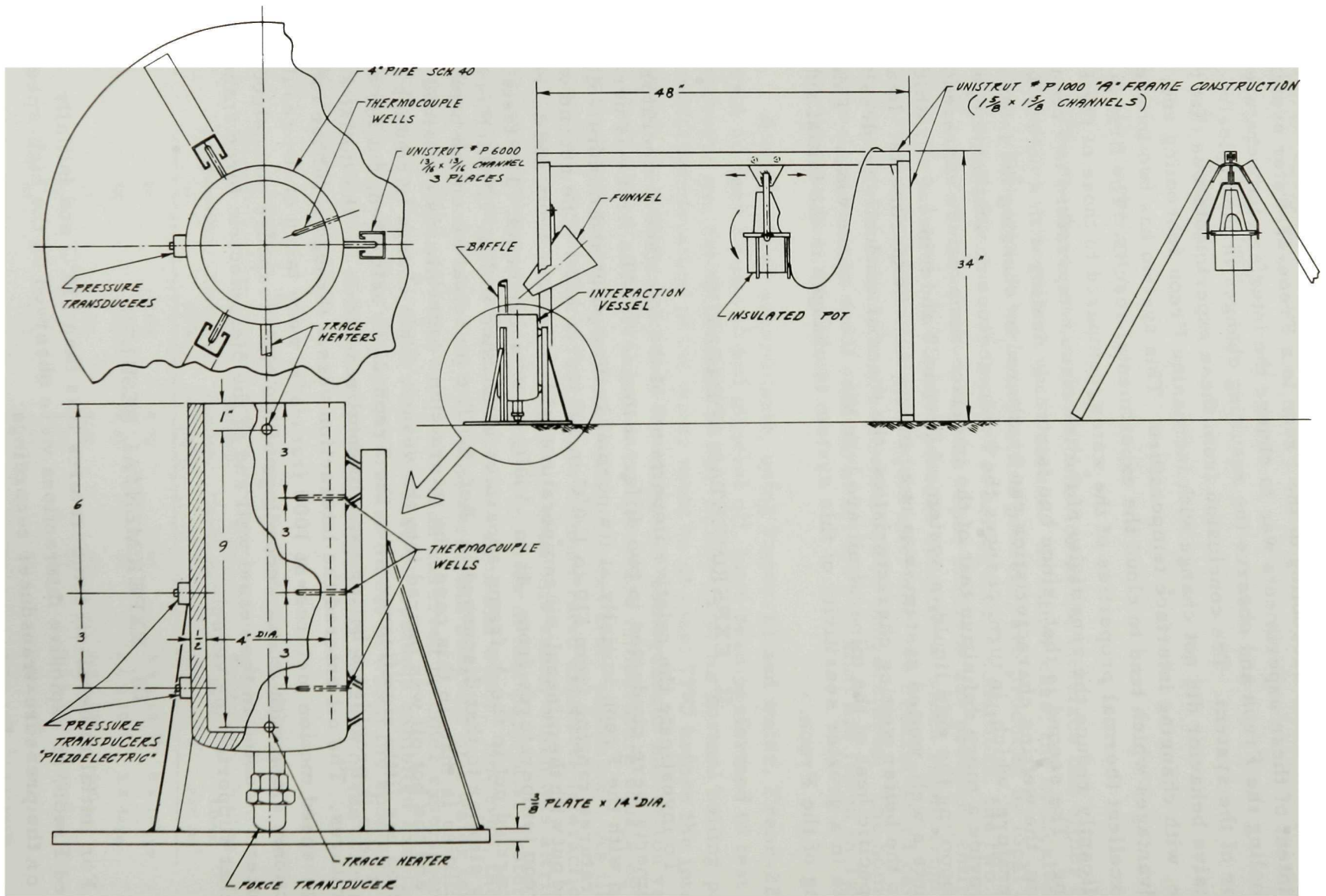


Fig. 1. Experimental Apparatus. All Dimensions in Inches. Conversion Factor: 1 in. = 2.54 cm. ANL Neg. No. 900-3067.

When the initial mineral-oil temperature was increased to 131°C, a vigorous expulsion of liquid was observed and the pressure transducers indicated a maximum pressure of 0.4 MPa (4 atm), but the rise time (see Fig. 2) was about 4 ms. However, a mineral-oil temperature of 140°C definitely provided an explosive interaction with a rise time less than 1 ms and a maximum interaction pressure of 0.6 MPa (6 atm), as shown in Fig. 3. Increasing interaction pressures were observed with increases in the mineral-oil temperature. For test conditions of saturated Freon and oil at 180°C, a small interaction was initially observed, and then a delay of 580 ms occurred before the large explosive event. The pressure trace for this run is shown in Fig. 4. The largest explosive interaction of the entire experimental sequence was observed with an initial oil temperature of 190°C and initially saturated Freon; as illustrated in Fig. 5, this event developed a maximum interaction pressure of 2 MPa (20 atm) with an extended decay characteristic.

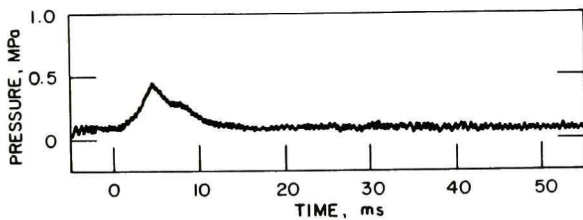


Fig. 2. Pressure-Time History for Freon-22 and Mineral-oil Undergoing Large-scale Interactions with  $T_{oil} = 131^{\circ}\text{C}$  and  $T_F = -41^{\circ}\text{C}$ . ANL Neg. No. 900-77-89 Rev. 1.

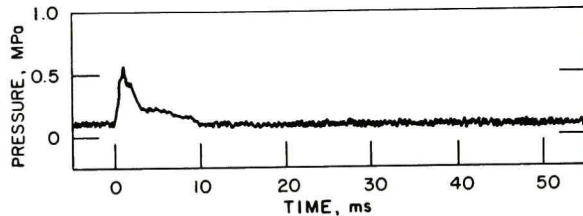


Fig. 3. Pressure-Time History for Freon-22 and Mineral-oil Undergoing Large-scale Interactions with  $T_{oil} = 140^{\circ}\text{C}$  and  $T_F = -41^{\circ}\text{C}$ . ANL Neg. No. 900-77-90 Rev. 1.

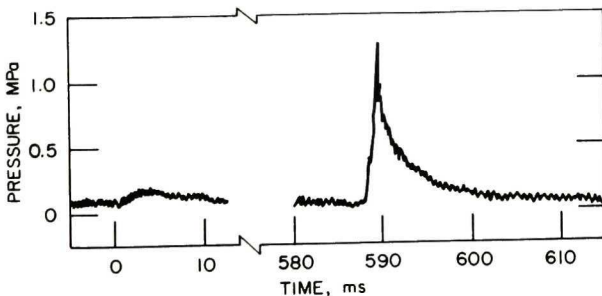


Fig. 4. Pressure-Time History for Freon-22 and Mineral-oil Undergoing Large-scale Interactions with  $T_{oil} = 180^{\circ}\text{C}$  and  $T_F = -41^{\circ}\text{C}$ . ANL Neg. No. 900-77-95 Rev. 1.

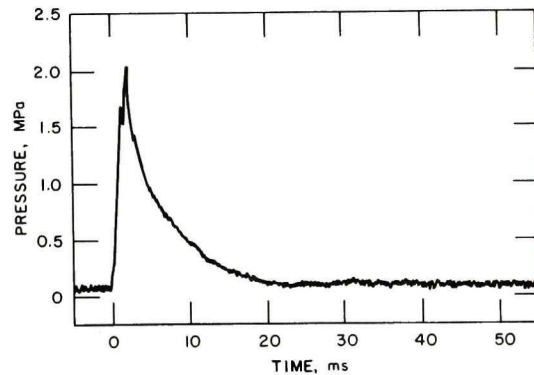


Fig. 5. Pressure-Time History for Freon-22 and Mineral-oil Undergoing Large-scale Interactions with  $T_{oil} = 190^{\circ}\text{C}$  and  $T_F = -41^{\circ}\text{C}$ . ANL Neg. No. 900-77-97 Rev. 1.

The second half of the test series was conducted with a constant initial oil temperature of  $190^{\circ}\text{C}$  and decreasing Freon temperatures. When the Freon was initially at  $-60^{\circ}\text{C}$ , a vigorous explosion was observed on the high-speed movies; the system pressure measurements are shown in Fig. 6. Two relatively small interactions were observed by 370 ms. For an initial Freon temperature of  $-80^{\circ}\text{C}$ , and the events were separated by 370 ms. For an initial Freon temperature of  $-100^{\circ}\text{C}$  the interaction pressure was 0.3 MPa (3 atm), as shown in Fig. 7. For initial Freon temperatures of  $-120$  and  $-140^{\circ}\text{C}$  and an initial mineral-oil temperature of  $190^{\circ}\text{C}$ , no explosive interactions were observed by any of the system instrumentation.

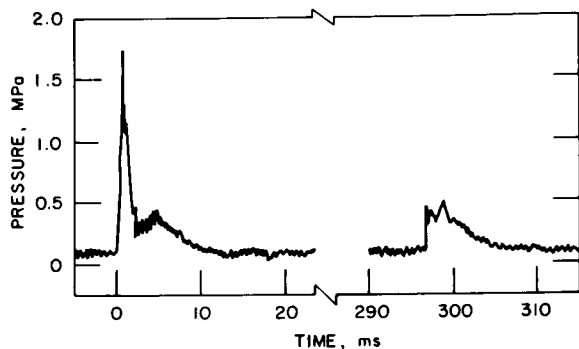


Fig. 6. Pressure-Time History for Freon-22 and Mineral-oil Undergoing Large-scale Interactions with  $T_{\text{oil}} = 190^{\circ}\text{C}$  and  $T_{\text{F}} = -60^{\circ}\text{C}$ . ANL Neg. No. 900-77-98 Rev. 1.

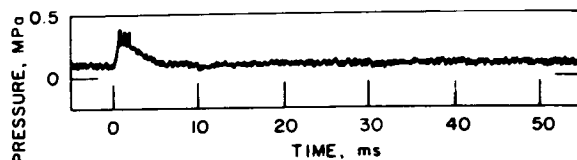


Fig. 7. Pressure-Time History for Freon-22 and Mineral-oil Undergoing Large-scale Interactions with  $T_{\text{oil}} = 190^{\circ}\text{C}$  and  $T_{\text{F}} = -100^{\circ}\text{C}$ . ANL Neg. No. 900-77-87 Rev. 1.

#### IV. DISCUSSION OF RESULTS

The initial conclusion that can be drawn from this set of experiments is that the explosive character of a given system can be suppressed by either cooling the hot liquid below a certain value or the cold liquid below a given level.

The original question of interest was whether the interface temperature provided an accurate method for evaluating the explosive potential of a given system. If a given interaction is simply considered as explosive or nonexplosive, regardless of its interaction pressure, the results can be plotted and compared to the idealized interface-temperature model in which the temperature for sustained explosive homogeneous nucleation is considered to be  $60^{\circ}\text{C}$ .<sup>2</sup> Such a representation is shown in Fig. 8 which demonstrates good agreement between the regions delineated as explosive and nonexplosive by the proposed model.

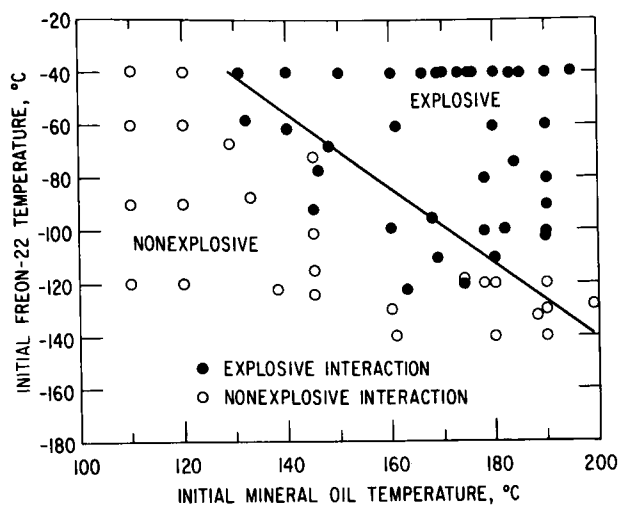


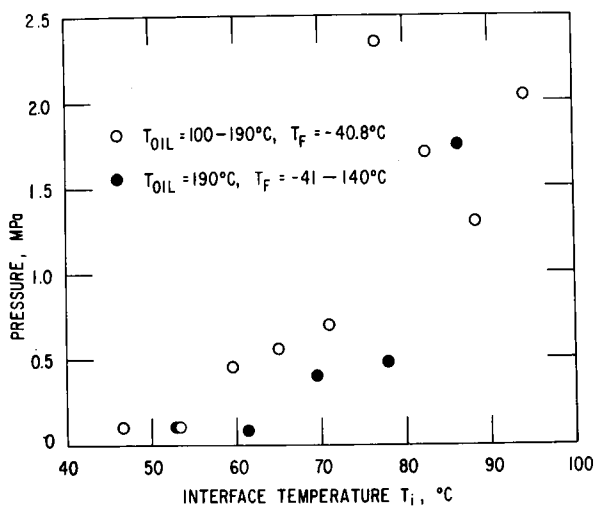
Fig. 8. Comparison between Interface-temperature Model and Experimental Results. ANL Neg. No. 900-75-289.

Additional experimental results were taken for various initial mineral-oil and Freon temperatures, and agreement was again obtained with the interface-temperature spontaneous-nucleation model. Some scatter is expected in the immediate region of the prediction as a result of changes in the subcooled Freon temperature when delays of several hundred milliseconds occur before the onset of explosive events. A  $40^{\circ}\text{C}$  change can be expected in the bulk temperature of a 1-mm-dia drop as a result of film-boiling heat transfer for 500 ms.

Another test of the interface-temperature model is to compare the explosive interaction pressures as a function of the system interface temperature, which is shown in Fig. 9 for the two parametric variations performed. When the broad range of thermal conditions treated is considered, the interface-temperature model provides an excellent means of describing the explosive characteristics of the system. Figure 10 displays the maximum interaction pressures for all the experiments as a function of the interface temperature.

The pressure and force measurements for the explosive tests are given in Appendix A. In some experiments, such as Run 6-11-75: 6 +145 -92, very sharp pressure spikes were measured at the initiation of the explosion. These spikes appeared to make little contribution to the work done by the explosion and could perhaps result from the impact of a liquid mass on a transducer face. This would be a definite consideration if the liquids are intimately dispersed prior to the event that both the high-speed movies and

Fig. 9  
Maximum Interaction Pressures as a Function of Interface Temperature.  
ANL Neg. No. 900-77-88 Rev. 1.



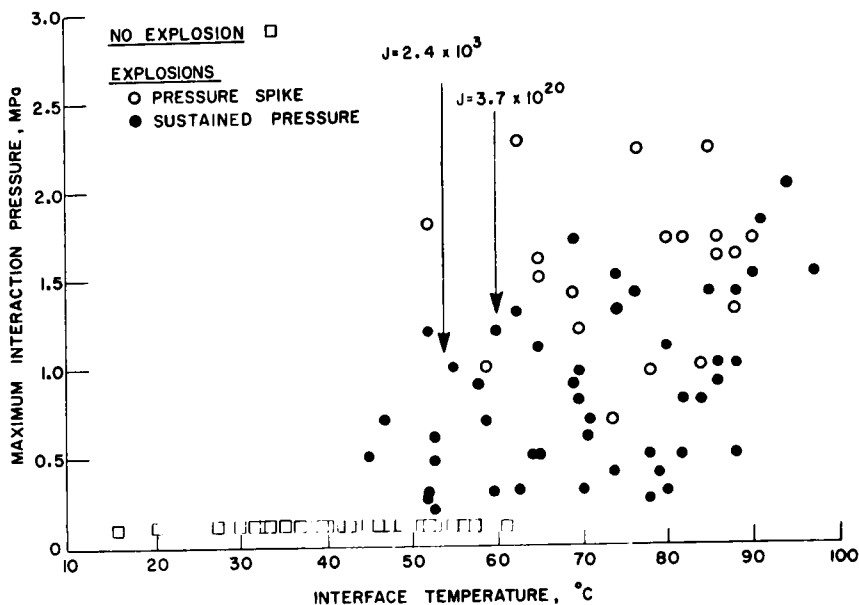


Fig. 10. Maximum Interaction Pressures vs Interface Temperature. ANL Neg. No. 900-77-76.

long delay times indicate is the case in these tests. Figure 10 shows the pressure spike and the sustained pressures (on a time scale of milliseconds), which are definitely doing work on the system. Although this illustration shows the same scatter in the vicinity of the threshold temperature as is shown in Fig. 8, it clearly shows the dramatic change in system behavior as the interface temperature changes by a few degrees.

## V. CONCLUSIONS

These experiments in this well-wetted system demonstrate that the interface temperature is a valid technique for characterizing the explosive potential of a given liquid pair.

## APPENDIX A

### Experimental Data

The experimental parameters and results are listed chronologically in Table II and the measurements for explosive events are given in Figs. A.1-A.47. The run numbers are structured to include the date, the test number on that date, the initial oil temperature, and the initial Freon temperature as shown below:

test number      initial Freon temperature (in °C)  
 ↓                    ↓  
8-1-75: 6 + 110 - 120  
 ↑                    ↑  
 date                initial oil temperature

TABLE II. Chronological List of Experiments

Run Number	Maximum Interactions Pressure, MPa	Note	Run Number	Maximum Interactions Pressure, MPa	Note
6-11-75: 1 +145 -72	1.50		7-17-75: 2 +190 -120	0	a
6-11-75: 2 +145 -124	0	a	7-17-75: 3 +190 -140	0	a
6-11-75: 3 +145 -115	0	a	7-18-75: 1 +190 -130	0	a
6-11-75: 4 +145 -101	0	a	7-18-75: 2 +190 -90	1.44	
6-11-75: 5 +148 -68	1.01		7-23-75: 1 +150 -41	0.68	
6-11-75: 6 +145 -92	1.22		7-23-75: 2 +170 -41	0.61	
6-16-75: 1 +169 -110	0.61	b	7-23-75: 3 +182 -99	1.55	
6-16-75: 2 +188 -132	0	a	7-23-75: 4 +190 -100	1.19	
6-16-75: 3 +174 -118	0	a	7-23-75: 5 +190 -80	1.01	
6-16-75: 4 +190 -111	1.69		7-24-75: 1 +190 -100	0.94	
6-16-75: 5 +146 -77	0.50		7-24-75: 2 +190 -80	0.27	
6-17-75: 1 +133 -87	0	a	7-24-75: 3 +190 -90	0.67	
6-17-75: 2 +140 -61	-	c	7-24-75: 4 +131 -41	0.34	
6-18-75: 1 +132 -58	0.19		7-24-75: 5 +120 -41	0	a
6-18-75: 2 +129 -67	0	a	7-24-75: 6 +110 -41	0	a
6-19-75: 1 +198 -128	0.48		7-25-75: 1 +180 -41	0.59	
6-19-75: 2 +184 -74	-	c	7-25-75: 2 +160 -41	2.41	
6-19-75: 3 +174 -120	0.23		7-25-75: 3 +180 -41	1.69	
6-19-75: 4 +168 -95	1.05		7-25-75: 4 +140 -41	0.59	
6-19-75: 5 +156 -94	0.44		7-25-75: 5 +195 -41	1.68	
7-10-75: 1 +160 -99	1.89		7-25-75: 6 +185 -41	2.04	
7-10-75: 2 +160 -140	0	a	7-25-75: 7 +175 -41	2.18	
7-10-75: 3 +138 -122	0	a	7-28-75: 1 +183 -41	1.69	
7-10-75: 4 +163 -122	0.50		7-28-75: 2 +176 -41	1.50	
7-10-75: 5 +160 -130	0	a	7-28-75: 3 +180 -41	1.24	
7-14-75: 1 +181 -140	0	a	7-28-75: 4 +173 -41	1.08	
7-14-75: 2 +178 -128	0	a	7-28-75: 5 +169 -41	1.78	
7-15-75: 1 +181 -120	0	a	7-28-75: 6 +166 -41	1.89	
7-15-75: 2 +180 -110	1.26		8-1-75: 1 +120 -60	0	a
7-15-75: 3 +178 -100	1.72		8-1-75: 2 +120 -90	0	a
7-15-75: 4 +178 -80	0.78		8-1-75: 3 +120 -120	0	a
7-15-75: 5 +180 -60	0.31	d	8-1-75: 4 +110 -60	0	a
7-15-75: 6 +161 -60	1.63		8-1-75: 5 +110 -90	0	a
7-16-75: 1 +190 -41	1.97		8-1-75: 6 +110 -120	0	a
7-16-75: 2 +190 -60	1.63		8-4-75: 3 +190 -100	0.25	
7-16-75: 3 +192 -80	0.41		8-4-75: 4 +190 -90	1.70	
7-17-75: 1 +190 -101	1.84				

aNo explosive event.

bForce-transducer data.

cExplosive event; no record.

dTop pressure-transducer data.

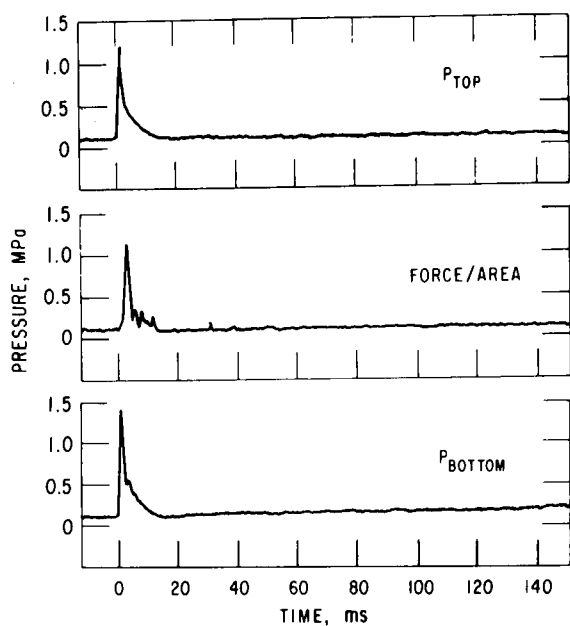


Fig. A.1. Experimental Data Records for  
Run 6-11-75: 1 +145 -72. ANL  
Neg. No. 900-76-371 Rev. 1.

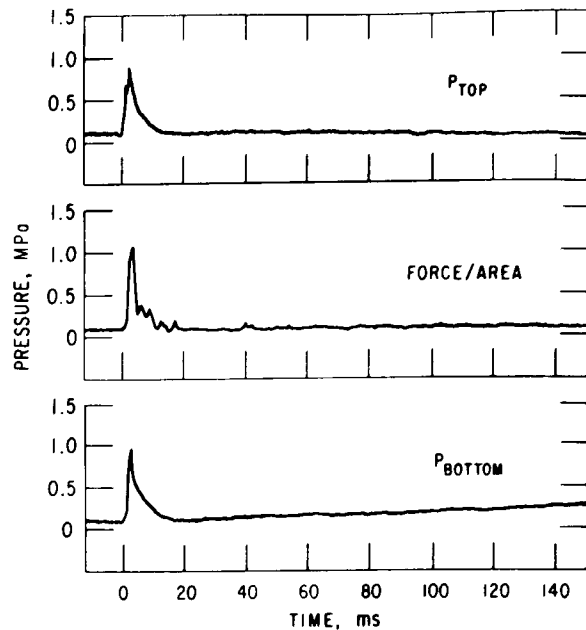


Fig. A.2. Experimental Data Records for  
Run 6-11-75: 5 +148 -68. ANL  
Neg. No. 900-76-384 Rev. 1.

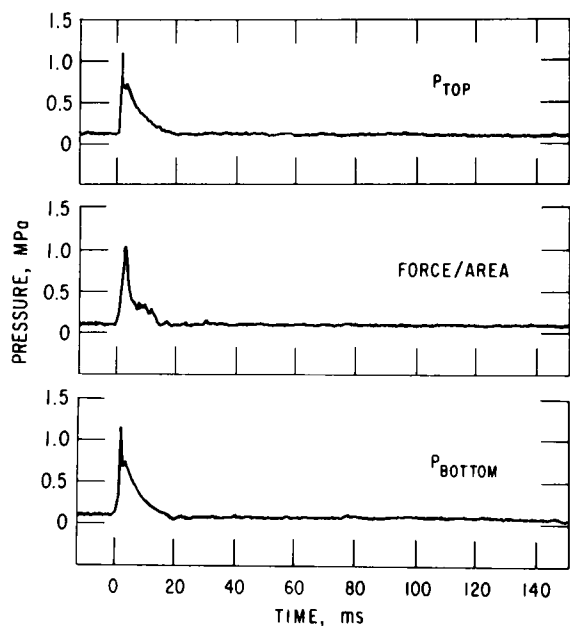


Fig. A.3. Experimental Data Records for  
Run 6-11-75: 6 +145 -92. ANL  
Neg. No. 900-76-358 Rev. 1.

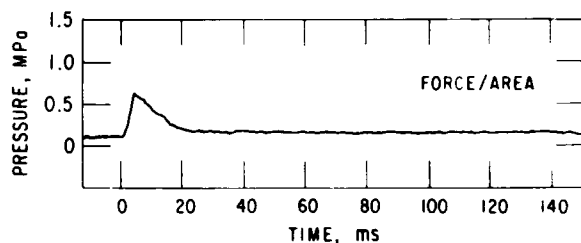


Fig. A.4. Experimental Data Records for  
Run 6-11-75: 1 +169 -110.  
(P<sub>bottom</sub> and P<sub>top</sub> not recorded).  
ANL Neg. No. 900-76-398 Rev. 1.

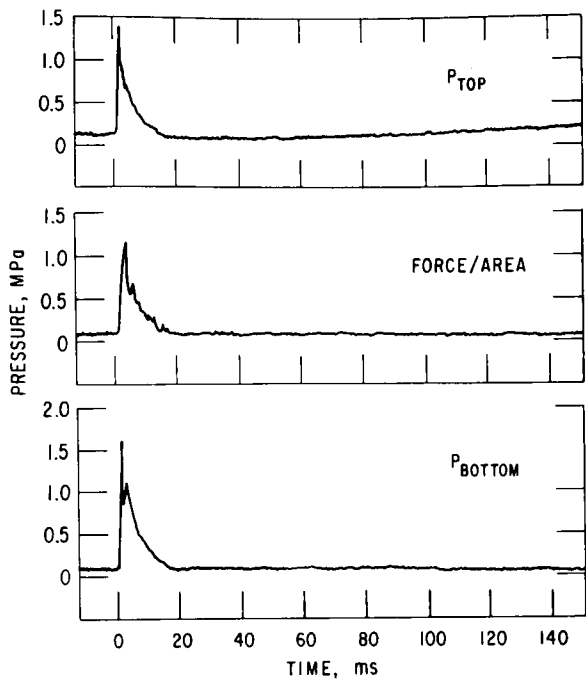


Fig. A.5. Experimental Data Records for  
Run 6-16-75: 4 +190 -111. ANL  
Neg. No. 900-76-355 Rev. 1.

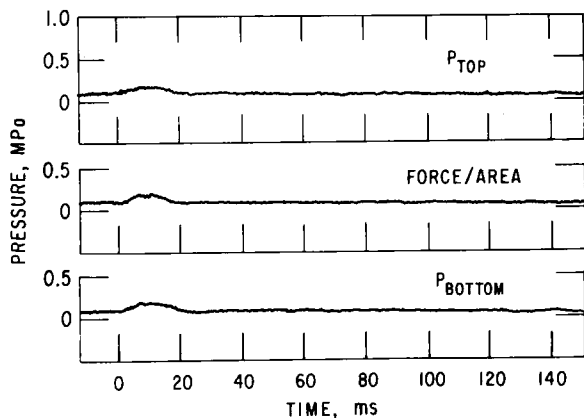


Fig. A.7. Experimental Data Records for  
Run 6-18-75: 1 +132 -58. ANL  
Neg. No. 900-76-361 Rev. 1.

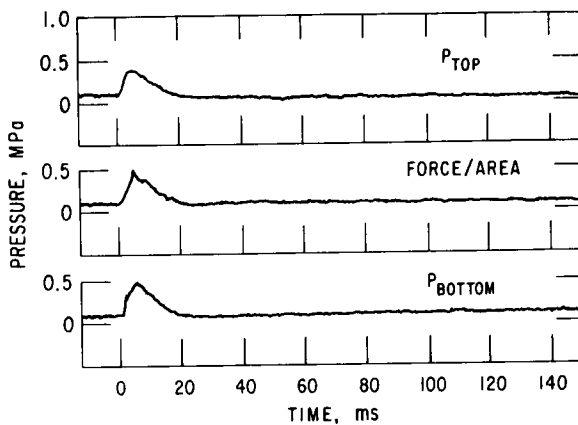


Fig. A.6. Experimental Data Records for  
Run 6-16-75: 5 +146 -77. ANL  
Neg. No. 900-76-386 Rev. 1.

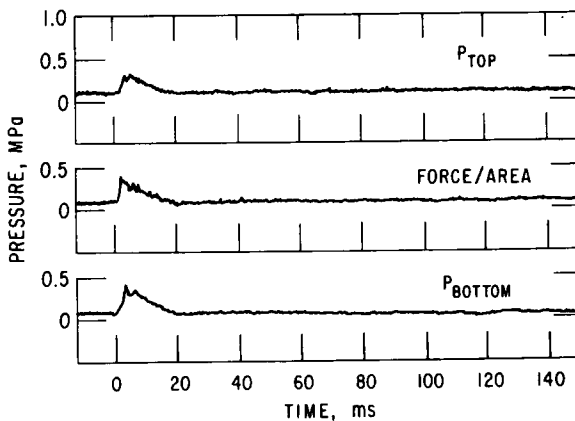


Fig. A.8. Experimental Data Records for  
Run 6-19-75: 1 +198 -128. ANL  
Neg. No. 900-76-379 Rev. 1.

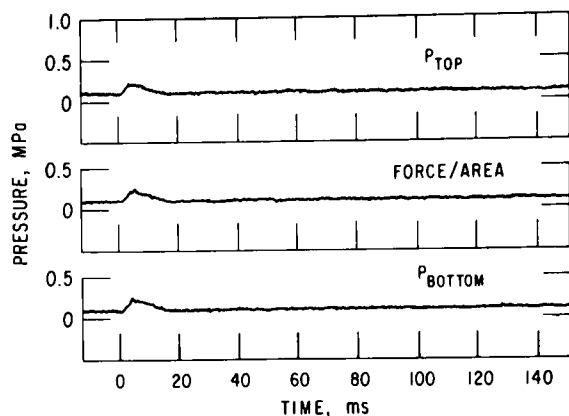


Fig. A.9. Experimental Data Records for  
Run 6-19-75: 3 +174 -120. ANL  
Neg. No. 900-76-388 Rev. 1.

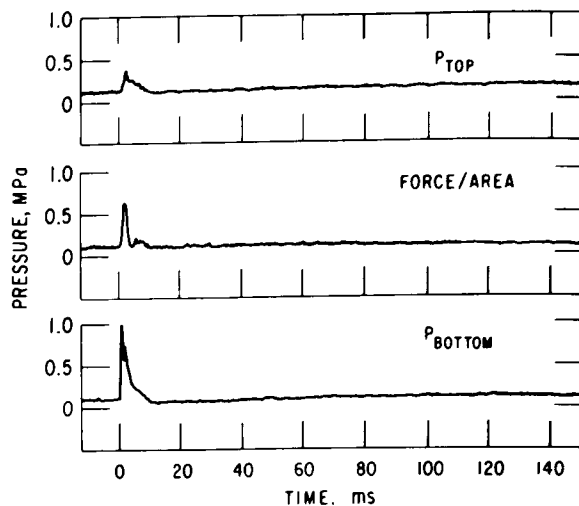


Fig. A.10. Experimental Data Records for  
Run 6-19-75: 4 +168 -95. ANL  
Neg. No. 900-76-364 Rev. 1.

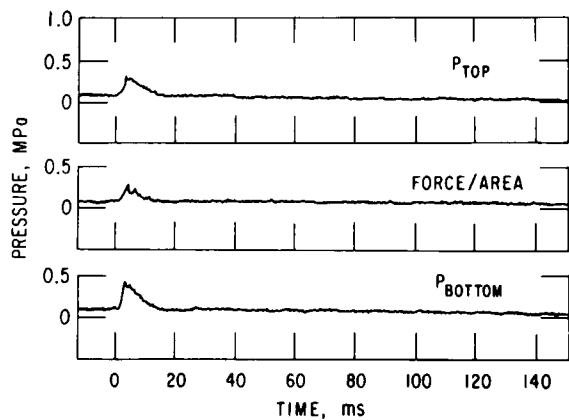


Fig. A.11. Experimental Data Records for  
Run 6-19-75: 5 +156 -94. ANL  
Neg. No. 900-76-368 Rev. 1.

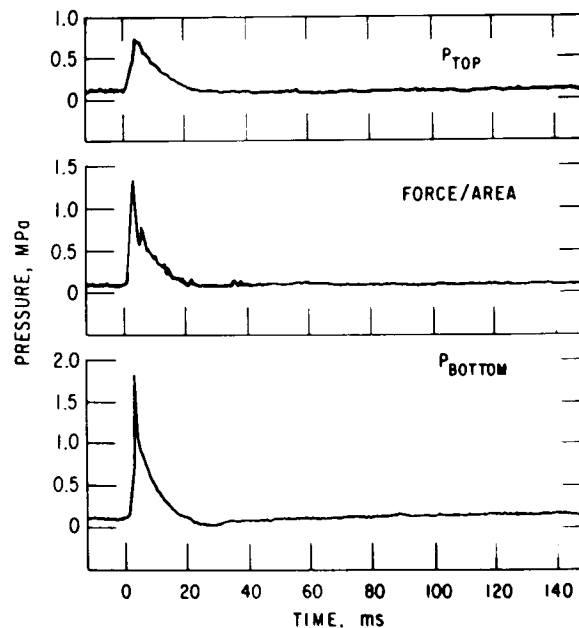


Fig. A.12. Experimental Data Records for  
Run 7-10-75: 1 +160 -99. ANL  
Neg. No. 900-76-366 Rev. 1.

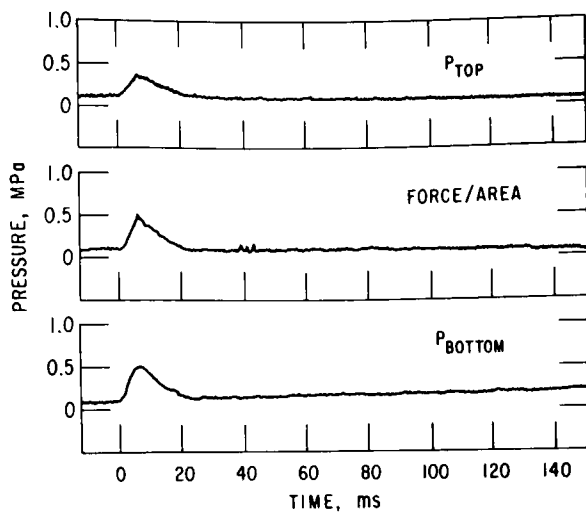


Fig. A.13. Experimental Data Records for  
Run 7-10-75: 4 +163 -122. ANL  
Neg. No. 900-76-389 Rev. 1.

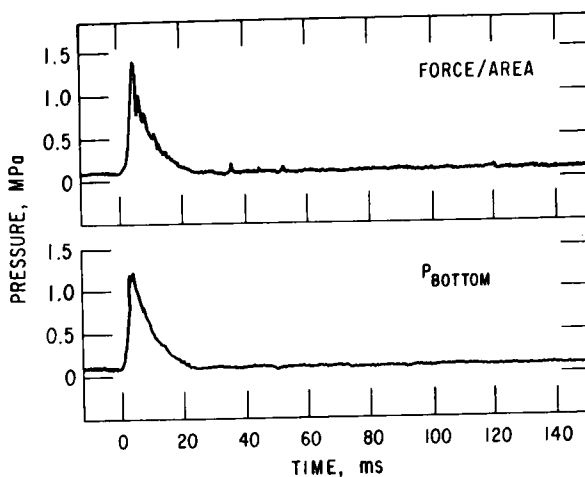


Fig. A.14. Experimental Data Records for  
Run 7-15-75: 2 +180 -110  
(P<sub>top</sub> not recorded). ANL Neg.  
No. 900-76-399 Rev. 1.

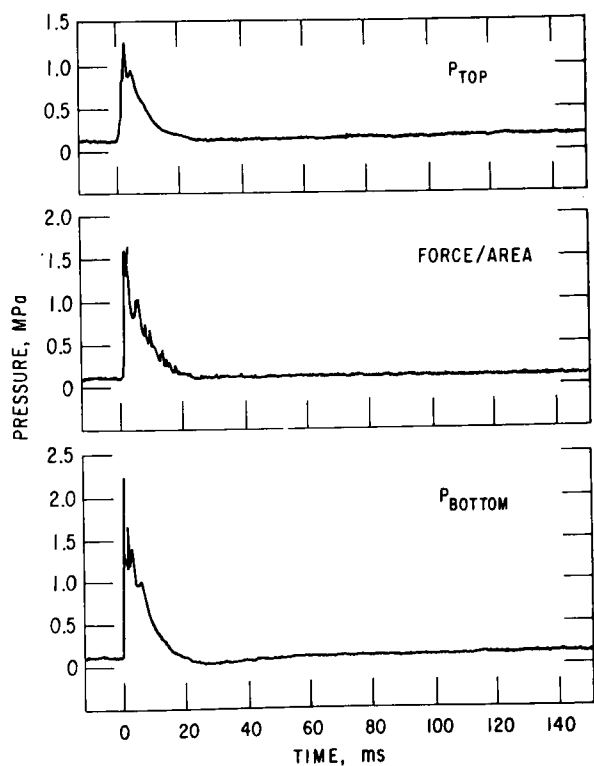


Fig. A.15. Experimental Data Records for  
Run 7-15-75: 3 +178 -100. ANL  
Neg. No. 900-76-357 Rev. 1.

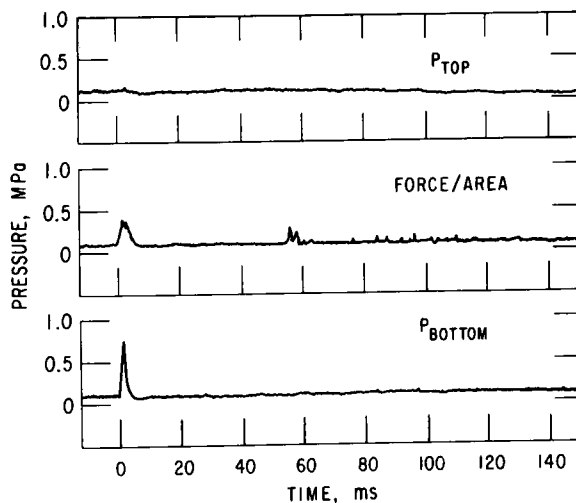


Fig. A.16. Experimental Data Records for  
Run 7-15-75: 4 +178 -80. ANL  
Neg. No. 900-76-363 Rev. 1.

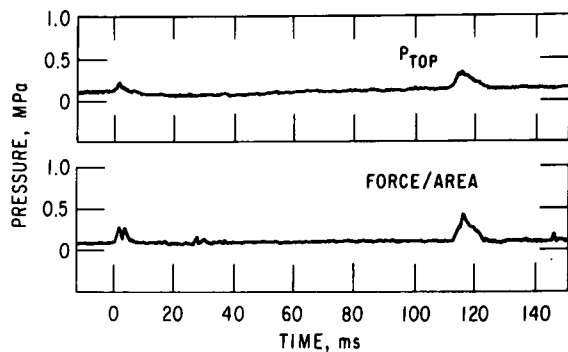


Fig. A.17. Experimental Data Records for  
Run 7-15-75: 5 +180 -60  
(P<sub>bottom</sub> not recorded). ANL  
Neg. No. 900-76-395 Rev. 1.

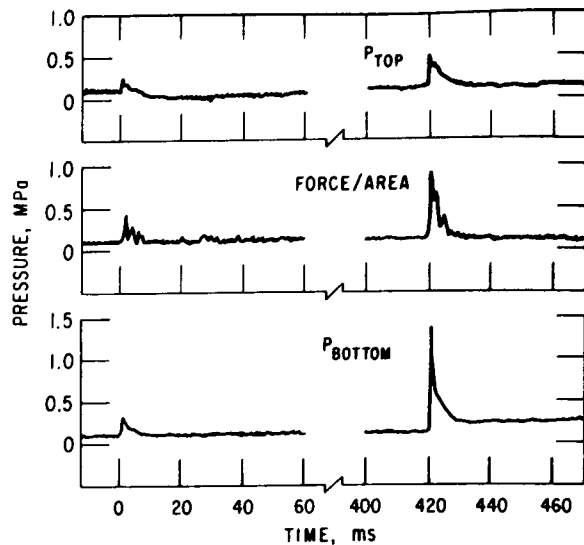


Fig. A.18. Experimental Data Records for  
Run 7-15-75: 6 +161 -60. ANL  
Neg. No. 900-76-383 Rev. 1.

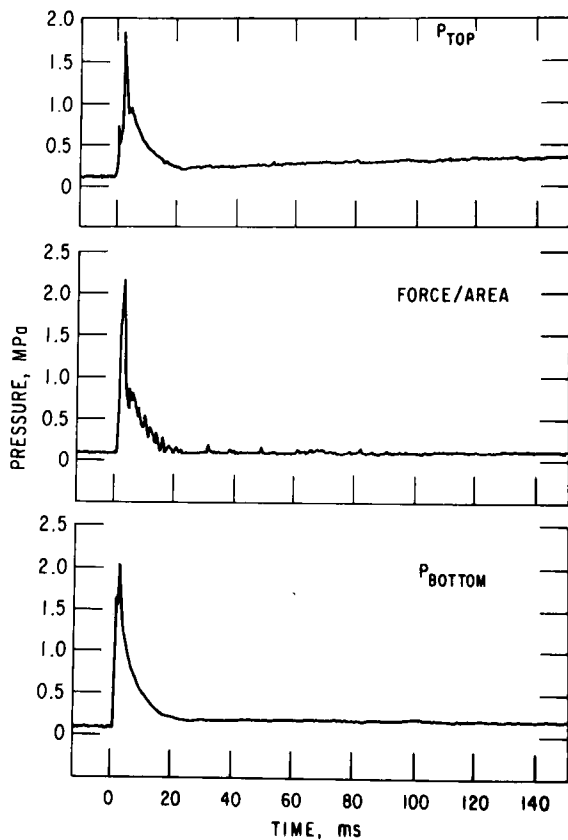


Fig. A.19. Experimental Data Records for  
Run 7-16-75: 1 +190 -41. ANL  
Neg. No. 900-76-356 Rev. 1.

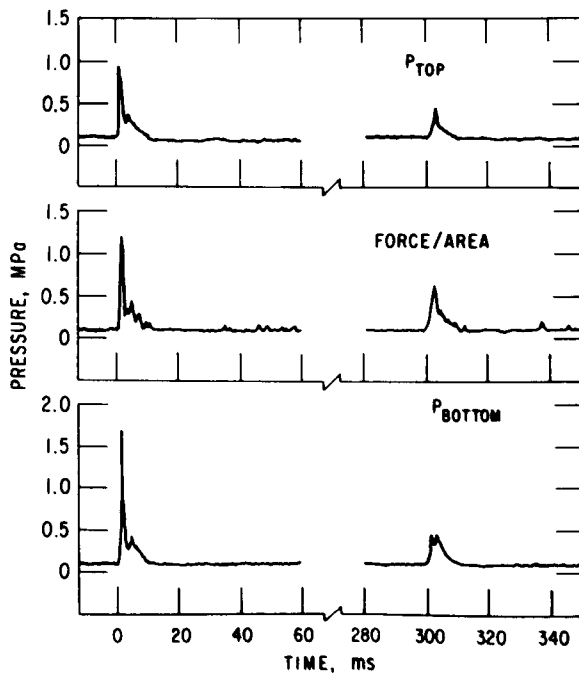


Fig. A.20. Experimental Data Records for  
Run 7-16-75: 2 +190 -60. ANL  
Neg. No. 900-76-380 Rev. 1.

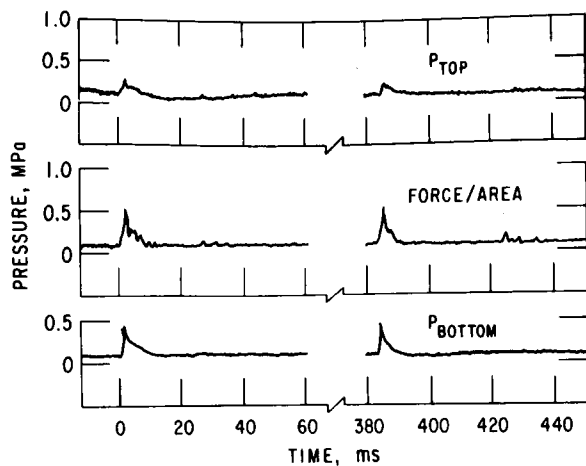


Fig. A.21. Experimental Data Records for  
Run 7-16-75: 3 +192 -80. ANL  
Neg. No. 900-76-394 Rev. 1.

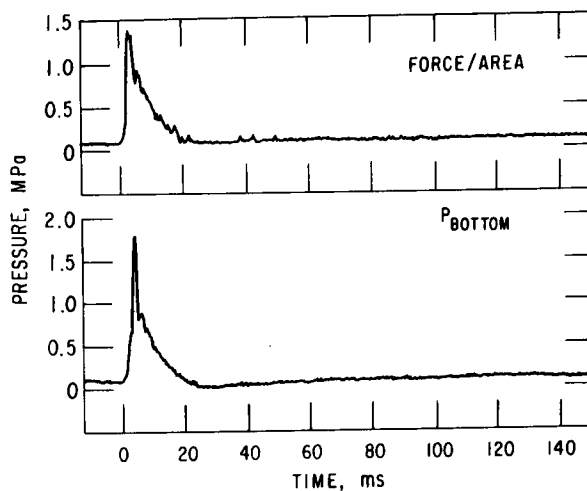


Fig. A.22. Experimental Data Records for  
Run 7-17-75: 1 +190 -101  
(P<sub>top</sub> not recorded). ANL Neg.  
No. 900-76-397 Rev. 1.

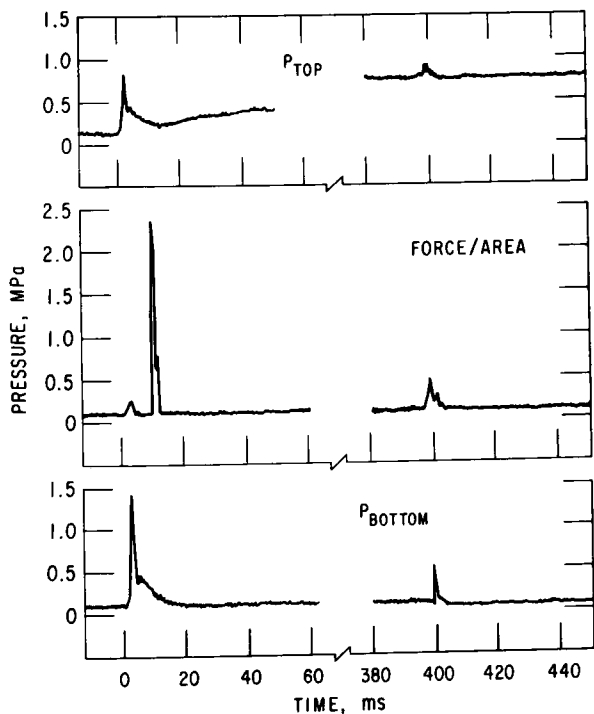


Fig. A.23. Experimental Data Records for  
Run 7-18-75: 2 +190 -90. ANL  
Neg. No. 900-76-354 Rev. 1.

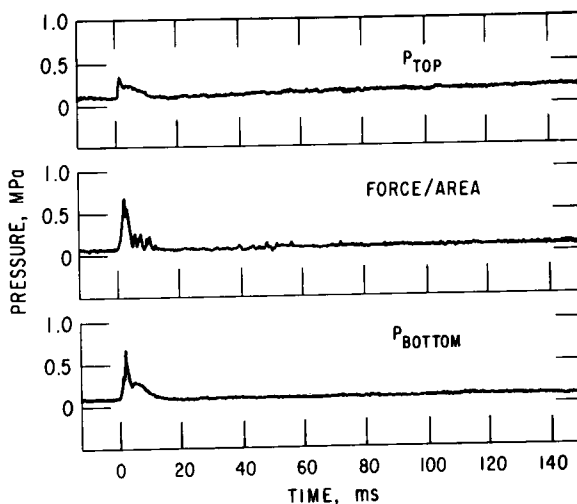


Fig. A.24. Experimental Data Records for  
Run 7-23-75: 1 +150 -41. ANL  
Neg. No. 900-76-387 Rev. 1.

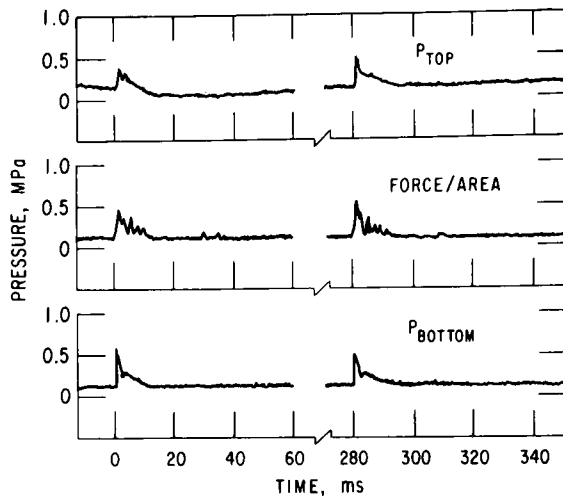


Fig. A.25. Experimental Data Records for  
Run 7-23-75: 2 +170 -41. ANL  
Neg. No. 900-76-381 Rev. 1.

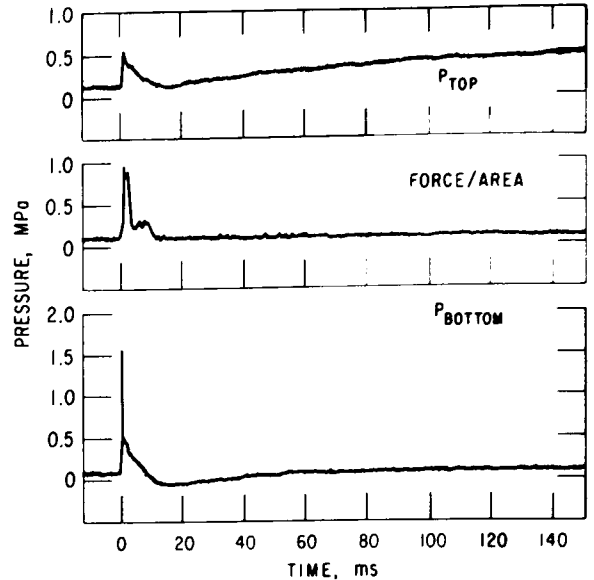


Fig. A.26. Experimental Data Records for  
Run 7-23-75: 3 +182 -99. ANL  
Neg. No. 900-76-359 Rev. 1.

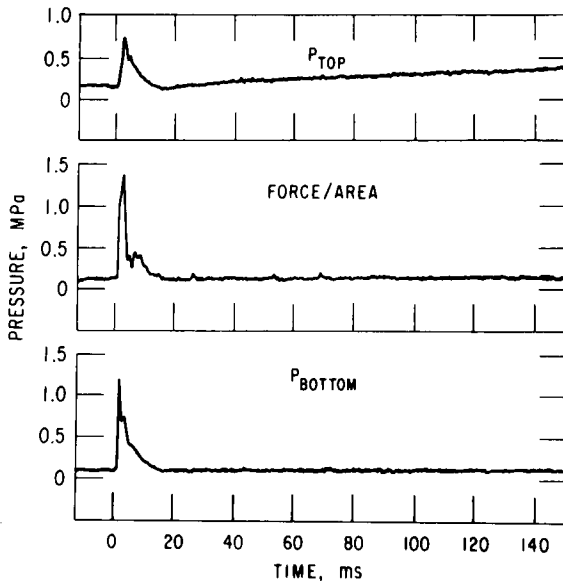


Fig. A.27. Experimental Data Records for  
Run 7-23-75: 4 +190 -100. ANL  
Neg. No. 900-76-375 Rev. 1.

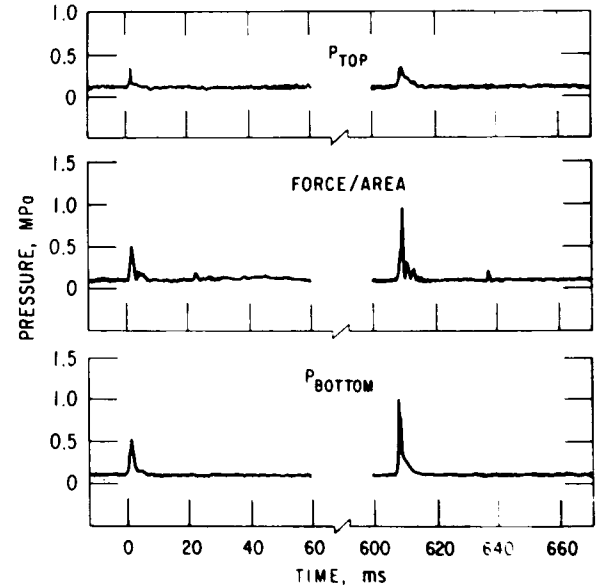


Fig. A.28. Experimental Data Records for  
Run 7-23-75: 5 +190 -80. ANL  
Neg. No. 900-76-382 Rev. 1.

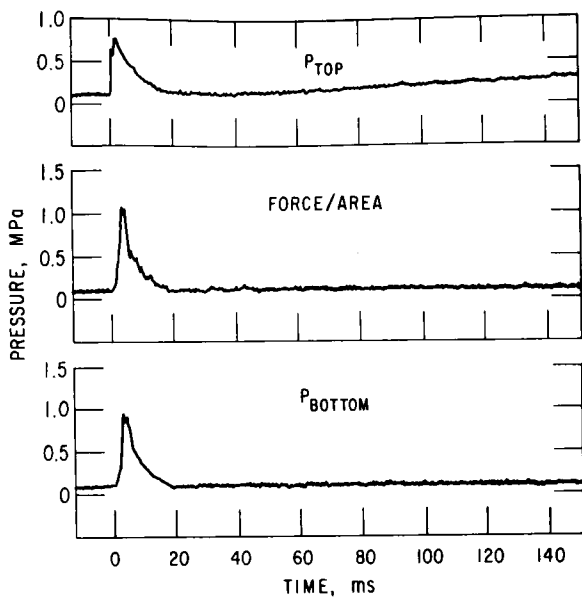


Fig. A.29. Experimental Data Records for  
Run 7-24-75: 1 +190 -100. ANL  
Neg. No. 900-76-369 Rev. 1.

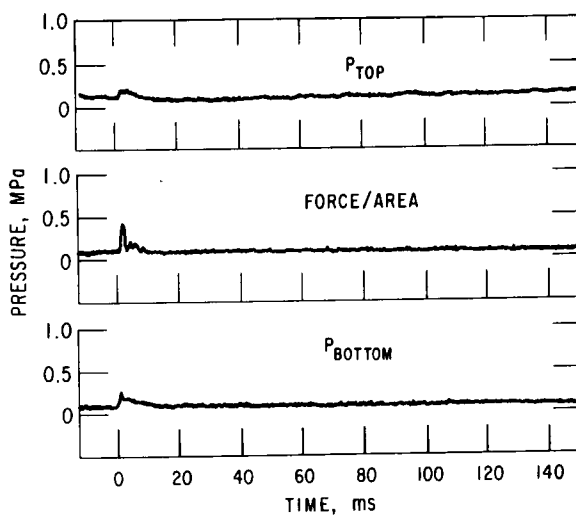


Fig. A.30. Experimental Data Records for  
Run 7-24-75: 2 +190 -80. ANL  
Neg. No. 900-76-362 Rev. 1.

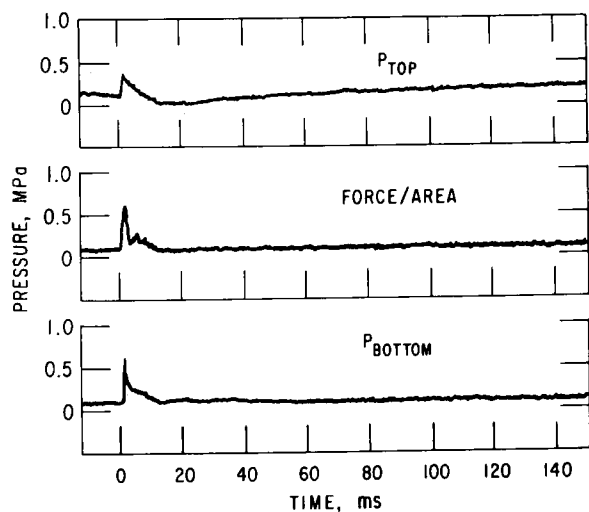


Fig. A.31. Experimental Data Records for  
Run 7-24-75: 3 +190 -90. ANL  
Neg. No. 900-76-377 Rev. 1.

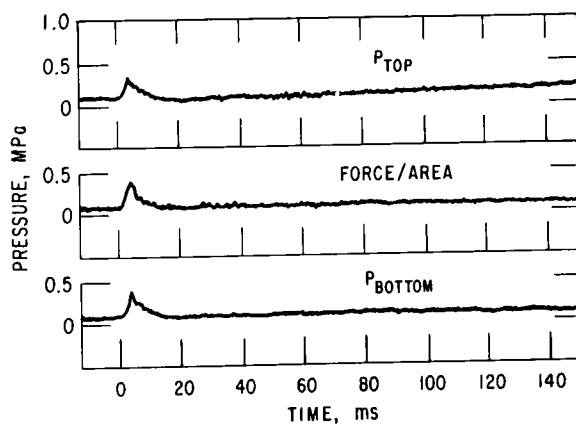


Fig. A.32. Experimental Data Records for  
Run 7-24-75: 4 +131 -41. ANL  
Neg. No. 900-76-385 Rev. 1.

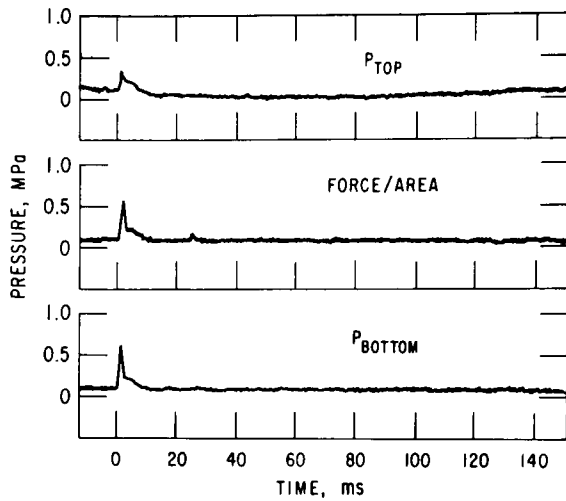


Fig. A.33. Experimental Data Records for  
Run 7-25-75: 1 +180 -41. ANL  
Neg. No. 900-76-378 Rev. 1.

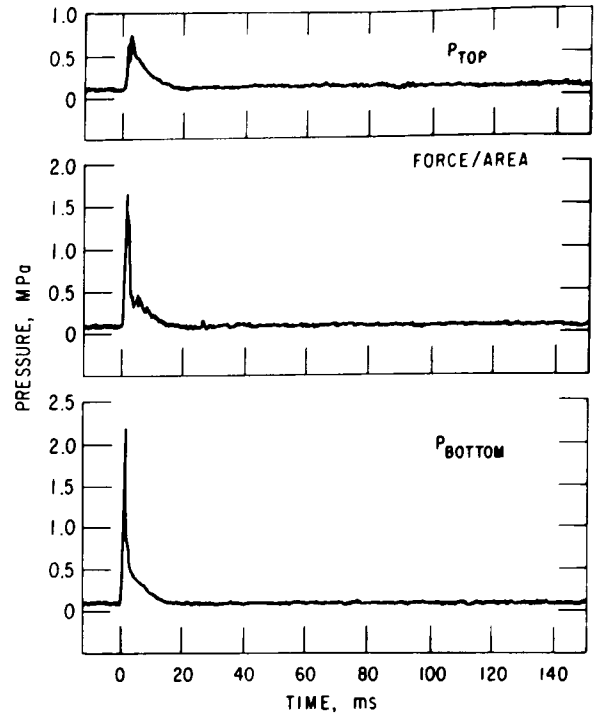


Fig. A.34. Experimental Data Records for  
Run 7-25-75: 2 +160 -41. ANL  
Neg. No. 900-76-392 Rev. 1.

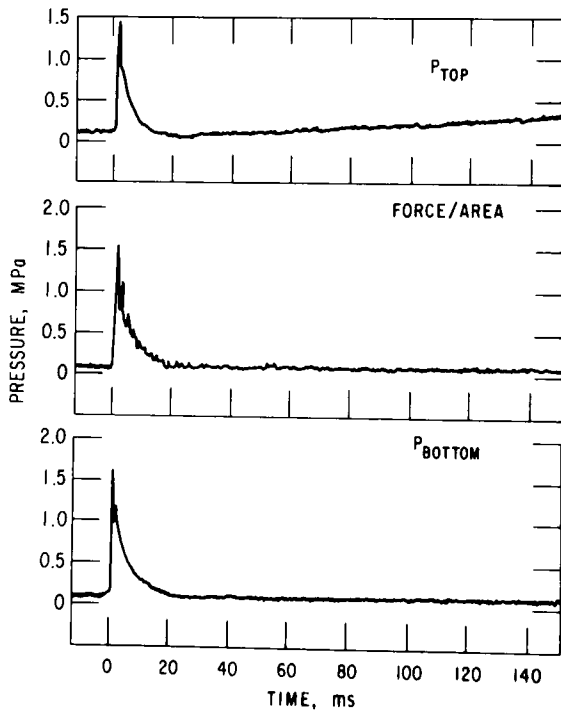


Fig. A.35. Experimental Data Records for  
Run 7-25-75: 3 +180 -41. ANL  
Neg. No. 900-76-365 Rev. 1.

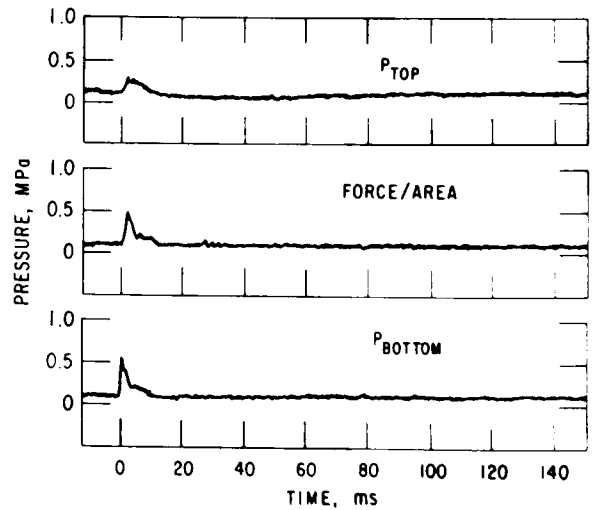


Fig. A.36. Experimental Data Records for  
Run 7-25-75: 4 +140 -41. ANL  
Neg. No. 900-76-376 Rev. 1.

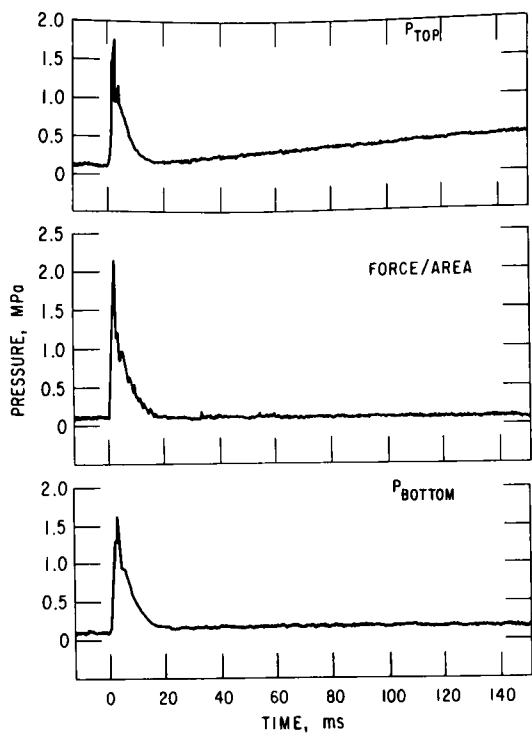


Fig. A.37. Experimental Data Records for  
Run 7-25-75: 5 +195 -41. ANL  
Neg. No. 900-76-391 Rev. 1.

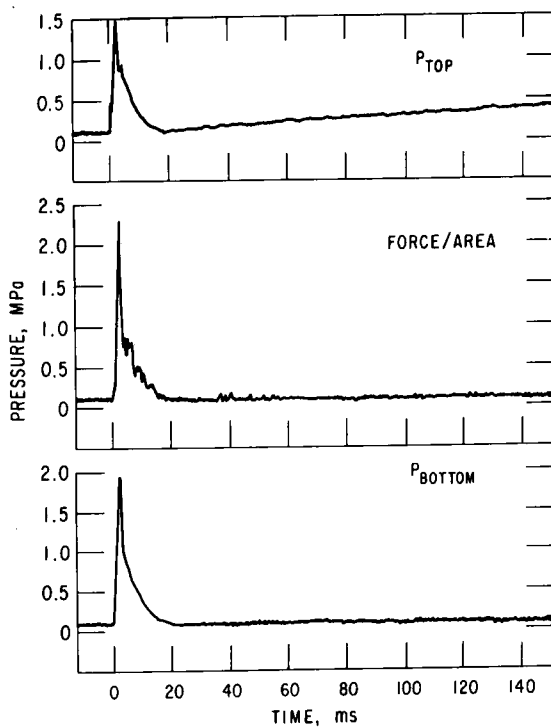


Fig. A.38. Experimental Data Records for  
Run 7-25-75: 6 +185 -41. ANL  
Neg. No. 900-76-360 Rev. 1.

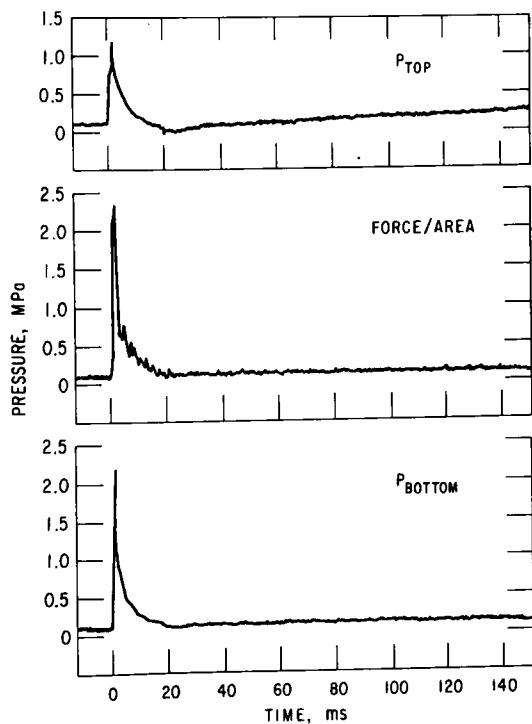


Fig. A.39. Experimental Data Records for  
Run 7-25-75: 7 +175 -41. ANL  
Neg. No. 900-76-393 Rev. 1.

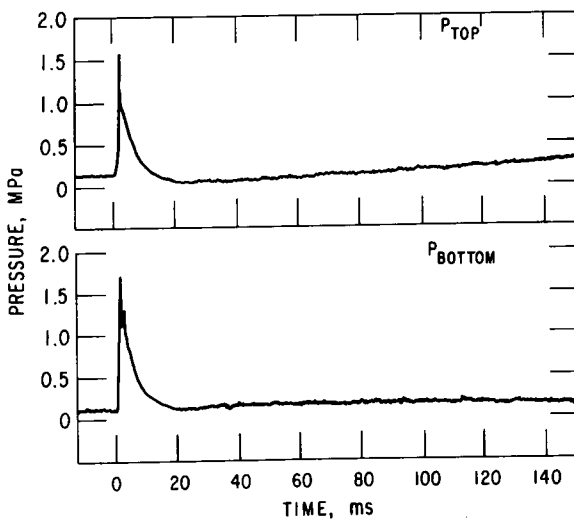


Fig. A.40. Experimental Data Records for  
Run 7-28-75: 1 +183 -41  
(Force/Area not recorded). ANL  
Neg. No. 900-76-396 Rev. 1.

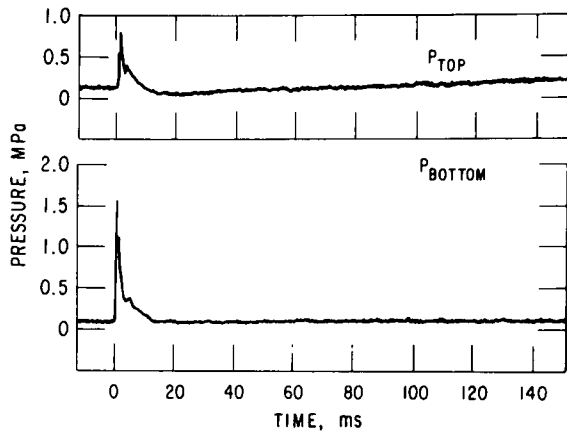


Fig. A.41. Experimental Data Records for  
Run 7-28-75: 2 +176 -41  
(Force/Area not recorded). ANL  
Neg. No. 900-76-400 Rev. 1.

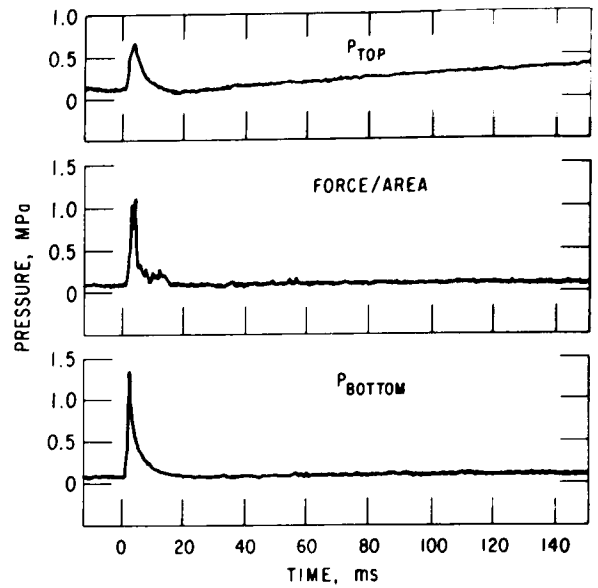


Fig. A.42. Experimental Data Records for  
Run 7-28-75: 3 +180 -41. ANL  
Neg. No. 900-76-372 Rev. 1.

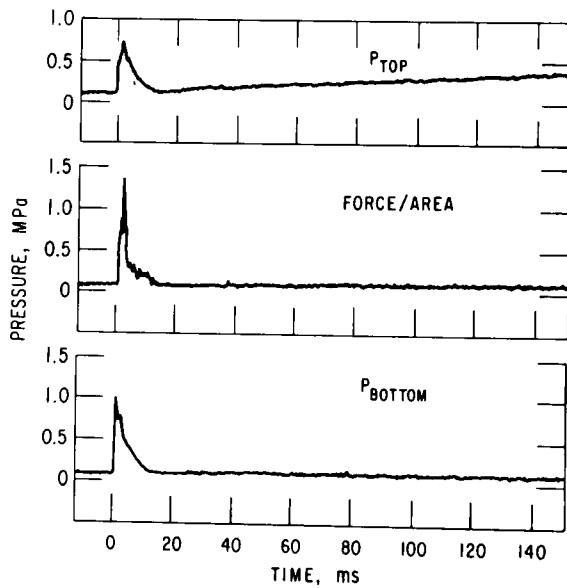


Fig. A.43. Experimental Data Records for  
Run 7-28-75: 4 +173 -41. ANL  
Neg. No. 900-76-370 Rev. 1.

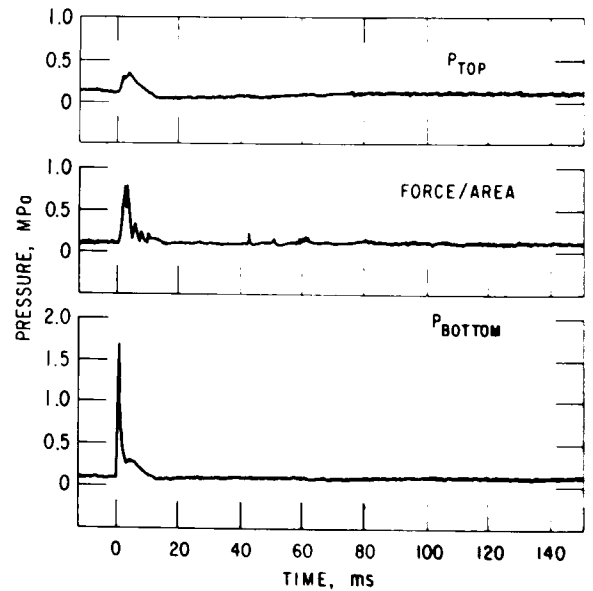


Fig. A.44. Experimental Data Records for  
Run 7-28-75: 5 +169 -41. ANL  
Neg. No. 900-76-367 Rev. 1.

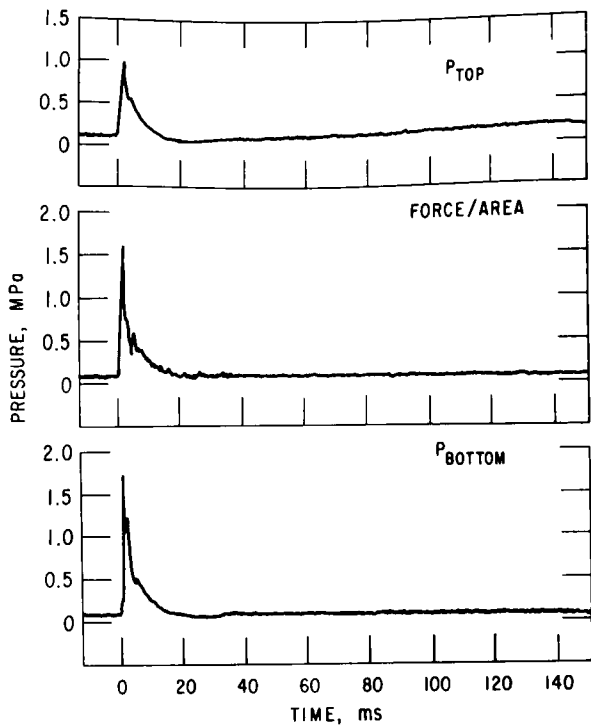


Fig. A.45. Experimental Data Records for  
Run 7-28-75: 6 +166 -41. ANL  
Neg. No. 900-76-373 Rev. 1.

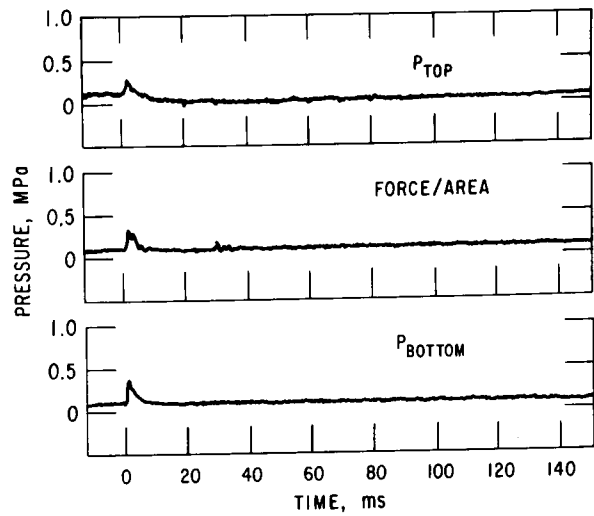


Fig. A.46. Experimental Data Records for  
Run 8-4-75: 3 +190 -100. ANL  
Neg. No. 900-76-374 Rev. 1.

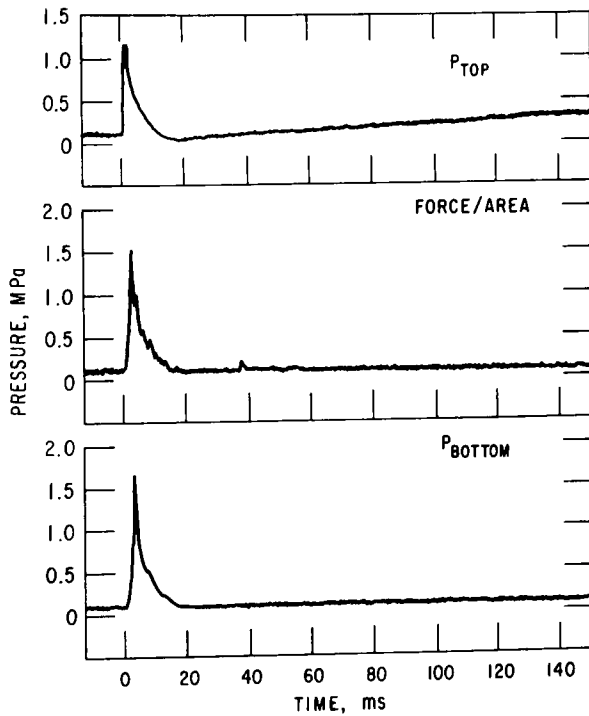


Fig. A.47  
Experimental Data Records for  
Run 8-4-75: 4 +190 -90. ANL  
Neg. No. 900-76-390 Rev. 1.

## APPENDIX B

## Results, Grouped by 10°C Increments of Oil Temperature

This appendix is a grouping of the experimental conditions by 10°C oil increments and includes contact interface temperatures for each test.

Run Number	T <sub>i</sub> , °C	P <sub>B</sub> , atm MPa	Note	Run Number	T <sub>i</sub> , °C	P <sub>B</sub> , atm MPa	Note
<u>110-119°C</u>				<u>Oil Temperature</u>			
8-1-75: 6 +110 -120	12	0	a	7-14-75: 2 +178 -118	42	0	a
8-1-75: 5 +110 -90	21	0	a	6-19-75: 3 +174 -120	43	0.23	
8-1-75: 4 +110 -60	34	0	a	6-16-75: 3 +174 -118	44	0	a
7-24-75: 6 +110 -41	43	0	a	7-15-75: 3 +178 -100	54	2.22	
<u>120-129°C</u>				<u>Oil Temperature</u>			
8-1-75: 3 +120 -120	13	0	a	7-15-75: 4 +178 -80	63	0.78	
8-1-75: 2 +120 -90	27	0	a	7-23-75: 2 +170 -41	72	0.61	
8-1-75: 1 +120 -60	40	0	a	7-28-75: 4 +173 -41	78	1.01	
6-18-75: 2 +129 -67	42	0	a	7-25-75: 7 +175 -41	79	2.18	
7-24-75: 5 +120 -41	48	0	a	7-28-75: 2 +176 -41	80	1.50	
<u>130-139°C</u>				<u>Oil Temperature</u>			
7-10-75: 3 +138 -122	22	0	a	<u>180-189°C</u>			
6-17-75: 1 +133 -87	35	0	a	7-14-75: 1 +181 -140	38	0	a
6-18-75: 1 +132 -58	48	0.19		6-16-75: 2 +188 -132	46	0	a
7-24-75: 4 +131 -41	55	0.34		7-15-75: 1 +181 -120	47	0	a
<u>140-149°C</u>				<u>Oil Temperature</u>			
6-11-75: 2 +145 -124	25	0	a	7-15-75: 2 +180 -110	51	1.26	
6-11-75: 3 +145 -115	29	0	a	7-23-75: 3 +182 -99	57	1.55	
6-11-75: 4 +145 -101	36	0	a	6-19-75: 2 +184 -74	69	-	b
6-11-75: 6 +145 -92	40	1.22		7-15-75: 5 +180 -60	73	0.31	e
6-16-75: 5 +146 -77	47	0.50		7-25-75: 1 +180 -41	82	0.59	
6-11-75: 1 +145 -72	49	1.50		7-25-75: 3 +180 -41	82	1.69	
6-11-75: 5 +148 -68	50	1.01		7-28-75: 3 +180 -41	82	1.29	
6-17-75: 2 +140 -61	51	-	b	7-28-75: 1 +183 -41	83	1.69	
7-25-75: 4 +140 -41	60	0.59		7-25-75: 6 +185 -41	85	2.04	
<u>150-159°C</u>				<u>Oil Temperature</u>			
6-19-75: 5 +156 -94	45	0.44		<u>190-199°C</u>			
7-23-75: 1 +150 -41	65	0.68		7-17-75: 3 +190 -140	43	0	a
<u>160-169°C</u>				<u>Oil Temperature</u>			
7-10-75: 2 +160 -140	27	0	a	7-18-75: 1 +190 -130	48	0	a
7-10-75: 5 +160 -130	31	0	a	7-17-75: 2 +190 -120	52	0	a
7-10-75: 4 +163 -122	36	0.50		6-19-75: 1 +198 -128	53	0.48	
7-10-75: 1 +160 -99	45	1.89		6-16-75: 4 +190 -111	56	1.69	
6-16-75: 1 +169 -110	45	0.61	c	7-17-75: 1 +190 -101	61	1.84	
6-19-75: 4 +168 -95	51	1.05		7-23-75: 4 +190 -100	61	1.19	
7-15-75: 6 +161 -60	63	1.63	d	7-24-75: 1 +190 -100	61	0.94	
7-25-75: 2 +160 -41	71	2.41		8-4-75: 3 +190 -100	61	0.25	
7-28-75: 6 +166 -41	74	1.89		7-18-75: 2 +190 -90	66	1.44	
7-28-75: 5 +169 -41	76	1.78		7-24-75: 3 +190 -90	66	0.67	
				8-4-75: 4 +190 -90	66	1.70	
				7-16-75: 4 +192 -80	70	0.41	
				7-23-75: 5 +190 -80	70	1.01	
				7-24-75: 2 +190 -80	70	0.27	
				7-16-75: 2 +190 -60	79	1.63	
				7-16-75: 1 +190 -41	87	1.97	
				7-25-75: 5 +195 -41	90	1.68	

<sup>a</sup>No explosive event.

<sup>b</sup>Explosive event; no record.

<sup>c</sup>Force-transducer data.

<sup>d</sup>Actual peak pressure, 1.63 MPa, not 1.37 MPa as shown.

<sup>e</sup>Top pressure-transducer data.

## REFERENCES

1. H. K. Fauske, *The Role of Nucleation in Vapor Explosions*, Trans. Am. Nucl. Soc. 15, 813 (1972).
2. R. E. Henry and H. K. Fauske, *Energetics of Vapor Explosions*, ASME Paper #75-HT-66 (1975).
3. H. S. Carslaw and J. C. Jaeger, *Conduction of Heat in Solids*, Second Edition, Clarendon Press, Oxford (1959).
4. V. P. Skripov, *Metastable Liquids*, Halstead Press, Jerusalem (1974).
5. R. E. Henry et al., "Large Scale Vapor Explosions," *Proc. Fast Reactor Safety Meet.*, Beverly Hills, CA, CONF-740401-P2, 922 (Apr 1974).
6. T. Enger and D. E. Hartman, *Mechanics of the LNG-Water Interaction*, Am. Gas Association Distribution Conf., Atlanta, GA (May 1972).
7. S. J. Board, R. W. Hall, and G. E. Brown, *The Role of Spontaneous Nucleation in Thermal Explosions: Freon/Water Experiments*, CEGB Report RD/B/N 3007 (1974).

Distribution for ANL-77-43Internal:

J. A. Kyger	I. Bornstein	L. M. Pavlik (5)
A. Amorosi	D. Rose	S. C. Yao
R. Avery	P. A. Lottes	L. M. McUmbert (10)
L. Burris	B. A. Korelc (4)	R. Gebner
D. W. Cissel	D. H. Lennox	D. R. Armstrong
S. A. Davis	M. J. McDaniel	L. Bova
B. R. T. Frost	J. B. Heineman	J. Santori
D. C. Rardin	L. W. Deitrich	E. A. Spleha
R. G. Staker	L. Baker	D. J. Quinn
R. J. Teunis	R. A. Noland	M. Farahat
C. E. Till	D. R. Ferguson	E. Gunchin
R. S. Zeno	R. P. Anderson	G. T. Goldfuss
C. E. Dickerman	K. I. Chang	E. G. Erickson
H. K. Fauske	W. L. Chen	J. C. Leung
S. Fistedis	D. H. Cho	A. Segev
B. D. LaMar	D. W. Condiff	B. W. Spencer
J. F. Marchaterre	M. Epstein	M. A. Grolmes
H. O. Monson	M. Ishii	A. B. Krisciunas
R. Sevy	G. A. Lambert	ANL Contract File
A. J. Goldman	T. C. Chawla	ANL Libraries (5)
E. L. Martinec	R. E. Henry (15)	TIS Files (4)

External:

ERDA-TIC, for distribution per UC-79p (282)  
 Manager, Chicago Operations Office  
 Chief, Chicago Patent Group  
 Director, ERDA-RDD (2)  
 Director, Reactor Programs Division, ERDA-CH  
 Director, CH-INEL  
 President, Argonne Universities Association  
 Reactor Analysis and Safety Division Review Committee:  
   W. Kerr, The Univ. Michigan  
   M. Levenson, Electric Power Research Inst.  
   S. Levy, General Electric Co., San Jose  
   R. B. Nicholson, Exxon Nuclear Co., Inc.  
   D. Okrent, Univ. California, Los Angeles

ARGONNE NATIONAL LAB WEST



3 4444 00011099 9

